Theor Appl Genet (2006) 113:783–799
DOI 10.1007/s00122-006-0321-3

ORIGINAL PAPER

Ty3/gypsy-like retrotransposon knockout of a 2-methyl-6-phytyl-1,4-benzoquinone methyltransferase is non-lethal, uncovers a cryptic paralogous mutation, and produces novel tocopherol (vitamin E) profiles in sunflower

Shunxue Tang · Catherine G. Hass · Steven J. Knapp

Received: 6 February 2006 / Accepted: 13 May 2006 / Published online: 9 August 2006

Abstract The *m* (*Tph*$_1$) mutation partially disrupts the synthesis of α-tocopherol (vitamin E) in sunflower (*Helianthus annuus* L.) seeds and was predicted to disrupt a methyltransferase activity necessary for the synthesis of α- and γ-tocopherol. We identified and isolated two 2-methyl-6-phytyl-1,4-benzoquinone/2-methyl-6-solanyl-1,4-benzoquinone methyltransferase (*MPBQ*/*MSBQ-MT*) paralogs from sunflower (*MT-1* and *MT-2*), resequenced *MT-1* and *MT-2* alleles from wildtype (m^+ m^+) and mutant (*m m*) inbred lines, identified *m* as a non-lethal knockout mutation of *MT-1* caused by the insertion of a 5.2 kb *Ty3/gypsy*-like retrotransposon in exon 1, and uncovered a cryptic codominant mutation (*d*) in a wildtype × mutant F_2 population predicted to be segregating for the *m* mutation only. *MT-1* and *m* cosegregated and mapped to linkage group 1 and *MT-1* was not transcribed in mutant homozygotes (*m m*). The *m* locus was epistatic to the *d* locus—the *d* locus had no effect in m^+ m^+ and m^+ *m* individuals, but significantly increased β-tocopherol percentages in *m m* individuals. *MT-2* and *d* cosegregated, *MT-2* alleles isolated from mutant homozygotes (*d d*) carried a 30 bp insertion at the start of the 5′-UTR, and *MT-2* was more strongly transcribed in seeds and leaves of wildtype (d^+ d^+) than mutant (*d d*) homozygotes (transcripts were 2.2- to 5.0-fold more abundant in the former than the latter). The double mutant (*m m d d*) was non-lethal and produced 24–45% α- and 55–74% β-tocopherol (the wildtype produced 96% α- and 4% β-tocopherol). *MT-2* compensated for the loss of the *MT-1* function, and the *MT-2* mutation profoundly affected the synthesis of tocopherols without adversely affecting the synthesis of plastoquinone crucial for normal plant growth and development.

Electronic Supplementary Material Supplementary material is available to authorised users in the online version of this article at http://dx.doi.org/10.1007/s00122-006-0321-3.

Communicated by C. Gebhardt

Shunxue Tang and Catherine G. Hass contributed equally to this work.

S. Tang · S. J. Knapp (✉)
Center for Applied Genetic Technologies,
The University of Georgia, 111 Riverbend Road,
Athens, GA 30602, USA
e-mail: sjknapp@uga.edu

C. G. Hass
Department of Crop and Soil Science,
Oregon State University, Corvallis,
OR 97331, USA

Introduction

Three loci (*m* = *Tph*$_1$, *g* = *Tph*$_2$, and *d*) are known to disrupt the synthesis of α-tocopherol (α-T) and produce novel tocopherol (vitamin E) profiles in sunflower (*Helianthus annuus* L.) seeds–wildtypes normally accumulate 92–98% α-T (Demurin 1993; Demurin et al. 1996; Hass et al. 2006). Loss-of-function *m*, *g*, and *d* mutations enhance the synthesis of other tocopherols and produce a broad spectrum of offtype tocopherol profiles in sunflower seeds. The *g* mutation knocks out a γ-tocopherol methyltransferase (γ-TMT) activity and causes the accumulation of > 90% γ-tocopherol (γ-T) in sunflower seeds (Hass et al. 2006). γ-*TMT* was normally transcribed and spliced in wildtype (g^+ g^+) inbred

lines, but weakly transcribed and alternatively spliced in mutant (*g g*) inbred lines (Hass et al. 2006). The activities disrupted by the *m* and *d* mutations are not known, but can be predicted from biochemical phenotypes produced by disrupting methyltransferase activities in the tocopherol biosynthetic pathway (Shintani and DellaPenna 1998; Porfirova et al. 2002; Shintani et al. 2002; Cheng et al. 2003; Collakova and DellaPenna 2001; Sattler et al. 2003, 2004).

Thus far, a single mutant *m* allele has been identified, is recessive and non-lethal, and partially disrupts the synthesis of α-T in sunflower seeds (Demurin 1993). The present study was undertaken to unravel the biochemical effects of the *m* locus independent of the *g* and *d* loci and identify the activity disrupted by and genetic mechanism underlying the *m* mutation. The biochemical phenotypes produced by the *m* locus and non-lethality of the *m* (mutant) allele (Demurin 1993; Demurin et al. 1996; Hass et al. 2006) are consistent with the partial disruption of an 2-methyl-6-phytyl-1,4-benzoquinone/2-methyl-6-solanyl-1,4-benzoquinone methyltransferase (MPBQ/MSBQ-MT) activity, particularly because null *MPBQ/MSBQ-MT* mutations disrupt plastoquinone (PQ) biosynthesis and are lethal in Arabidopsis (Cheng et al. 2003). The recessivity of the *m* allele, however, is consistent with a null or near-null *MPBQ/MSBQ-MT* mutation. Loss-of-function *MPBQ/MSBQ-MT* mutations are predicted to disrupt flow through the 2,3-dimethyl-6-phytyl-1,4-benzoquinone (DMPBQ) ⇒ γ-T ⇒ α-T branch of the pathway, redirect flow through the MPBQ ⇒ δ-tocopherol (δ-T) ⇒ β-tocopherol (β-T) branch of the pathway, and enhance the synthesis and accumulation of δ- and β-T (Cheng et al. 2003; Motohashi et al. 2003; Van Eenennaam et al. 2003).

Fortuitously, a cryptic mutation (*d*) segregated in the wildtype × mutant (NMS373 × SRA16) population we developed for mapping the *m* locus (NMS373 × SRA16 was predicted to be segregating for the *m* mutation only). The mutant allele (*d*) was not identified in earlier phenotypic analyses of the *m* and *g* mutations (Demurin 1993; Demurin et al. 1996). The biochemical phenotypes produced by the *d* locus and non-lethality of the *d* (mutant) allele in populations segregating for *g* and *d* mutations (Hass et al. 2006) are consistent with the partial disruption of an MPBQ/MSBQ-MT activity (Cheng et al. 2003). *d* locus mutations were first discovered by Hass et al. (2003, 2006) in segregating populations (B109 × LG24 and R112 × LG24) developed for mapping the *g* locus (both were originally predicted to be homozygous for the *m* mutation and segregating for the *g* mutation). Neither was predicted to be segregating for *d* mutations. Hass et al. (2003, 2006) mapped the *d* locus to linkage group 4 and *g* locus to linkage group 8 and identified *m*, *d*, and *g* locus genotypes needed for mapping the *m* locus, isolating single, double, and triple mutants, and unravelling intragenic and intergenic effects among the three loci. Here, we describe the isolation of *MPBQ/MSBQ-MT* paralogs (*MT-1* and *MT-2*) and genetic mapping of *MT-1* and *MT-2* loci in a population segregating for *m* and *d* mutations (NMS373 × SRA16), identify MPBQ/MSBQ-MT activities disrupted by the *m* and *d* mutations, unravel the mystery behind the *d* locus, and trace the origin of cryptic, partial loss-of-function *d* alleles. Further, we describe the intragenic and intergenic effects of *MT-1* and *MT-2*, nucleotide diversity among *MT-1* and *MT-2* alleles, sequence-tagged-site (STS) markers diagnostic for wildtype and mutant *MT-1* and *MT-2* alleles, and novel tocopherol profiles produced in sunflower seeds by *MT-1* and *MT-2* mutations.

Materials and methods

Genetic stocks and segregating populations

Sunflower inbred lines (SRA16, MB17, HG81, HD55, VHG8, VHB18, and VHB45) carrying mutant *m*, *g*, or *d* alleles or combinations thereof were developed by phenotypic selection and single-seed-descent (SSD) among F_2, F_3, and F_4 progeny from assorted crosses (Table 1). SRA16, MB17, HG81, and HD55 were developed from R112/LG24. Hass et al. (2006) developed R112. Demurin (1993) developed LG24. We produced single-cross hybrids (NMS373/F_2-81 and NMS373/F_2-17) by crossing male-sterile (ms_{10} ms_{10}) NMS373 individuals to male-fertile (Ms_{10} Ms_{10}) R112/LG24 F_2 individuals (F_2-81 and F_2-17, respectively). NMS373 is a wildtype inbred line (Table 1), segregates for a recessive nuclear male-sterility gene (ms_{10}), and is near-isogenic to RHA373 (Miller 1997; Perez-Vich et al. 2005). F_2 seeds were produced by manually selfing one hybrid individual from each cross. VHG8 was developed from NMS373/F_2-81. VHB18 and VHB45 were developed from NMS373/F_2-17 (Table 1). NMS373 × SRA16 F_2 seeds were produced by manually selfing a single hybrid individual from a cross between NMS373 and SRA16 F_3-16-2, a single F_3 individual (*m m* g^+ g^+ d^+ d^+) developed from a cross between R112 and LG24 (Hass et al. 2006; Table 1). Genetic analyses were performed on two additional wildtype inbred lines, RHA280 (PI 552943; Fick et al. 1974) and RHA801 (PI 599768; Roath et al. 1981). F_1, F_2, F_3, F_4, F_5, and inbred line seeds were harvested

Table 1 Tocopherol profiles, pedigrees, and putative *m*, *g*, and *d* locus genotypes for wildtype and mutant F_2 individuals and inbred lines

Source[a]	Pedigree	Genotype	Tocopherol (% ± SE)			
			α	β	γ	δ
NMS373	Miller (1997)	$m^+ m^+ g^+ g^+ d\ d$	95.8 ± 2.5	4.2 ± 2.5	0.0 ± 0.0	0.0 ± 0.0
RHA280	Fick et al. (1974)	$m^+ m^+ g^+ g^+ d\ d$	94.1	3.0	2.9	0.0
RHA801	Roath et al. (1981)	$m^+ m^+ g^+ g^+ d\ d$	96.7	3.3	0.0	0.0
F_2-16	R112/LG24	$m\ m\ g^+ g^+ d^+ d^+$	87.5	12.5	0.0	0.0
F_3-16-2	F_2-16	$m\ m\ g^+ g^+ d^+ d^+$	88.9	4.2	6.9	0.0
SRA16 F_5	F_3-16-2	$m\ m\ g^+ g^+ d^+ d^+$	88.5 ± 1.7	8.8 ± 1.4	2.8 ± 1.6	0.0 ± 0.0
F_1	NMS373/F_3-16-2	$m^+\ m\ g^+ g^+ d^+ d$	88.8	7.5	3.8	0.0
F_2-81	R112/LG24	$m\ m\ g\ g\ d^+ d^+$	0.0	0.0	92.9	7.1
HG81 F_5	F_2-81	$m\ m\ g\ g\ d^+ d^+$	3.7 ± 3.4	0.0 ± 0.0	82.7 ± 5.0	13.6 ± 7.6
F_2-8	NMS373/ F_2-81	$m^+ m^+ g\ g\ d^+ d^+$	0.0	0.0	95.9	4.1
VHG8 F_3	F_2-8	$m^+ m^+ g\ g\ d^+ d^+$	0.3 ± 0.8	0.0 ± 0.0	95.2 ± 1.1	4.6 ± 0.9
F_2-17	R112/LG24	$m\ m\ g^+ g^+ d\ d$	41.7	58.3	0.0	0.0
MB17 F_5	F_2-17	$m\ m\ g^+ g^+ d\ d$	42.0 ± 10.3	57.7 ± 10.4	0.0 ± 0.0	0.3 ± 0.7
F_2-18	NMS373/ F_2-17	$m\ m\ g^+ g^+ d\ d$	21.1	77.8	1.1	0.0
VHB18 F_3	F_2-18	$m\ m\ g^+ g^+ d\ d$	30.3 ± 7.1	69.7 ± 7.1	0.0 ± 0.0	0.0 ± 0.0
F_2-45	NMS373/ F_2-17	$m\ m\ g^+ g^+ d\ d$	17.9	81.2	0.0	1.8
VHB45 F_3	F_2-45	$m\ m\ g^+ g^+ d\ d$	24.0 ± 4.1	74.1 ± 4.1	0.0 ± 0.0	1.9 ± 0.7
F_2-55	R112/LG24	$m\ m\ g\ g\ d\ d$	0.0	0.0	40.0	60.0
HD55 F_5	F_2-55	$m\ m\ g\ g\ d\ d$	0.0 ± 0.0	0.0 ± 0.0	32.7 ± 2.8	67.3 ± 2.8

[a] F_1 and F_2 individuals selected for developing inbred lines and segregating populations (NMS373 × SRA16 F_3-16-2 and F_2-8, 16, 17, 18, 45, 55, and 81) were phenotyped using half-seed samples. RHA280 and RHA801 were phenotyped using a single bulked seed sample

from greenhouse-grown plants (16 h photoperiod and 19–27°C temperature range). Seeds and plants were handled and DNA and RNA samples were isolated as described by Hass et al. (2006).

Isolation of *MPBQ/MSBQ-MT* paralogs

BLAST searches of the Compositate Genome Program Database (CGPdb; http://cgpdb.ucdavis.edu/) and National Center for Biotechnology Information (NCBI) GenBank Databases (http://www.ncbi.nlm.nih.gov/) were performed using cDNA and amino acid sequences for Arabidopsis *MPBQ/MSBQ-MT* (Genbank accession No. AB0542571 and At3g63410; Cheng et al. 2003; Motohashi et al. 2003) as query templates to identify sunflower *MPBQ/MSBQ-MT* homologs. Putative *MPBQ/MSBQ-MT* ESTs identified in the initial search were subsequently used as query templates in BLAST searches and identified several additional sunflower ESTs homologous to Arabidopsis *MPBQ/MSBQ-MT* (Cheng et al. 2003; Motohashi et al. 2003). *MT-1* and *MT-2* cDNA ends were isolated using 5′ and 3′ rapid amplification of cDNA ends (RACE) on developing seed RNAs (25-DAF) isolated from NMS373, R112, LG24, RHA280, and RHA801. RACE-PCR analyses were performed using the FirstChoice RLM-RACE kit and protocol (Ambion Inc., Austin, TX, USA). We isolated the 5′ ends of *MT-1* cDNAs by two rounds of nested RACE-PCR using R39 as the inner and R41 as the outer primer, the 3′ ends of *MT-1* cDNAs by two rounds of nested RACE-PCR using a single primer (F58), the 5′ ends of *MT-2* cDNAs by two rounds of nested RACE-PCR using R9 as the inner and R11 as the outer primer, and the 3′ ends of *MT-2* cDNAs by two rounds of nested RACE-PCR using F18 as the inner and F16 as the outer primers.

Full-length *MT-1* and *MT-2* cDNA sequences were isolated from NMS373, R112, LG24, RHA280, and RHA801 using reverse transcription (RT) PCR and sequenced on ABI 3730 or 3730 XL DNA Analyzers (Applied Biosystems, Foster City, CA, USA). Full-length *MT-1* and *MT-2* genomic DNA sequences were subsequently isolated by sequencing amplicons produced by long-distance (LD) PCR, essentially as described by Cheng et al. (1994), using AccuPrime High Fidelity Taq DNA Polymerase (Invitrogen Life Technology, Carlsbad, CA, USA), an initial denaturation step at 94°C for 2 min, 36 cycles at 94°C for 25 s, 58°C for 30 s, and 68°C for 4.5 min, and a final extension step at 68°C for 20 min.

DNA and amino sequences were aligned and statistical analyses were performed using ClustalW (http://www.ebi.ac.uk/clustalw/; Thompson et al. 1994) and GeneDoc 2.6 (http:// www.psc.edu/biomed/genedoc/). Synonymous and non-synonymous SNPs, other DNA

polymorphisms, and haplotypes were identified and nucleotide and haplotype diversity statistics were estimated using DnaSP 4.0 (http://www.ub.es/dnasp/; Rozas et al. 2003). Tandem and inverted repeat and hairpin sequences were identified using Blast 2 (http://www.ncbi.nlm.nih.gov/blast/bl2seq/wblast2.cgi; Tatusova and Madden 1999). *MT-1* and *MT-2* genomic DNA sequences were screened for the presence of transposable elements using The Institute for Genomic Research (TIGR) Plant Repeat Database (http://www.tigr.org/tdb/e2k1/ plant.repeats/) and Genetic Information Research Institute (GIRI) Repeat Element Database (http://www.girinst.org/censor/index.html). Conserved domains in a long-terminal-repeat (LTR) retrotransposon found in an *MT-1* allele were identified using the NCBI Conserved Domain Database (http://www.ncbi.nlm.nih.gov/Structure/cdd; Marchler-Bauer and Bryant 2004).

MT-1 and *MT-2* expression analyses

RT-PCR analyses of *MT-1* and quantitative RT-PCR (qRT-PCR) analyses of *MT-2* expression were performed on 60-DAG leaf and 25-DAF developing seed RNAs isolated from wildtype and mutant inbred lines using paralog specific primers (F38/R57 for *MT-1* and F10/R14 for *MT-2*) and protocols and methods described by Hass et al. (2006). qRT-PCR analyses of *MT-2* expression were performed in triplicate using actin (GenBank Acc. No. AF282624) for normalization. Standard curves were produced for *MT-2* and actin using 32, 16, 8, 4, and 2 ng of total RNA isolated from developing seeds (25-DAF) and 64, 32, 16, 8, and 4 ng of total RNA isolated from leaves (60-DAG). *MT-2* transcript accumulation was normalized to actin using comparative threshold (C_t) values calculated by the Opticon Monitor Analysis Software (MJ Research Inc., Waltham, MA, USA).

Phenotyping, genotyping, genetic mapping, and quantitative genetic analyses

Bulked segregant analyses (BSA), genotyping and genetic mapping of biochemical, simple sequence repeat (SSR), and insertion–deletion (INDEL) marker loci, HPLC phenotyping of tocopherols, and quantitative genetic analyses of the effects of *MT-1* and *MT-2* loci on α-, β-, γ-, and δ-T percentages were performed as described by Hass et al. (2006); 190 NMS373 × SRA16 F_2 progeny were phenotyped and genotyped. HPLC analyses were performed on total lipids isolated from half-seed samples of the 190 F_2 progeny (lipids were isolated from the upper half of each F_2 seed). The lower half of each F_2 seed was germinated and transplanted into 1.8 l pots filled with sandy loam soil.

Bulked-segregant analyses (Michelmore et al. 1991) were performed on DNA samples produced by bulking 10 individuals each from the upper and lower tails of the α-T distribution among NMS373 × SRA16 F_2 progeny; *m* locus genotypes of F_2 individuals selected from the upper and lower tails were predicted to be m^+m^+ and *m m*, respectively. NMS373, SRA16, and m^+m^+ and *m m* bulks were screened for length polymorphisms using previously mapped SSR markers (Tang et al. 2002, 2003). INDEL markers were developed for *MT-1* and *MT-2* and were screened for length polymorphisms among several mutant and wildtype inbred lines on ethidium-bromide stained agarose gels. Once SSR marker loci linked to the *m* locus were identified, *MT-1* and *MT-2* INDEL markers and several linkage group 1 SSR markers were genotyped among 190 NMS373 × SRA16 F_2 progeny and *m*, *d*, *MT-1*, *MT-2*, and SSR marker loci were grouped and ordered using MAPMAKER (Lander et al. 1987), essentially as described by Tang et al. (2002) and Hass et al. (2006). The *MT-1* locus was mapped in the RHA280 × RHA801 RIL mapping population ($n = 94$ RILs) by genotyping *MT-1* INDEL markers and reordering the *MT-1* locus and SSR marker loci on linkage group 1 (Tang et al. 2002, 2003).

Statistical analyses and SAS PROC GLM (Statistical Analysis System, Cary, NC; http:// www.sas.com) programs identical to those described by Hass et al. (2006) were used to estimate additive (A), dominance (D), A × A, A × D, D × A, and D × D effects of *MT-1* and *MT-2* on α-, β-, γ-, and δ-T percentages among NMS373 × SRA16 F_2 progeny, the coefficient of determination (R^2) for the complete 3^2 factorial (two-locus) model (eight degrees of freedom), and other statistics.

Databases searches for *MPBQ/MSBQ-MT* homologs

MT-1 and *MT-2* cDNA and amino acid sequences were used as query templates in BLAST searches of NCBI GenBank nucleotide, EST, and protein databases to identify *MPBQ/MSBQ-MT* homologs in other plants. Chloroplast transit peptides (CTPs) were predicted using ChloroP 1.1 (http://www.cbs.dtu.dk/services/ChloroP/; Emanuelsson et al. 1999). Conserved *S*-adenosyl methionine binding domains (SAM I, II, and III) found in *S*-adenosyl methionine-dependent methyltransferases (Kagan and Clarke 1994; Joshi and Chiang 1998) were identified in the sunflower *MPBQ/MSBQ-MT* amino acid sequence alignment. DNA and protein sequences were aligned using ClustalW

with default parameter settings (http://www.ebi.ac.uk/clustalw/; Thompson et al. 1994).

Results

Transmission of a cryptic mutation (*d*) by the wildtype parent in an F_2 population segregating for the *m* mutation

The NMS373 × SRA16 F_2 population was developed for forward genetic analyses and genetic mapping of the *m* locus by selfing a single hybrid individual from a cross between NMS373 and SRA16 F_3-16-2 (Fig. 1; Table 1). NMS373 had a wildtype tocopherol profile (95.8% α-T) and was predicted to be homozygous for wildtype *m*, *g*, and *d* alleles (m^+ m^+ g^+ g^+ d^+ d^+), whereas SRA16 F_3-16-2 produced slightly less α-T than NMS373 (88.9% α-T) and was predicted to be homozygous for wildtype *g* and *d* and mutant *m* alleles (*m m* g^+ g^+ d^+ d^+). The tocopherol profile for the hybrid was nearly identical to the female parent (SRA16 F_3-16-2) (Fig. 1; Table 1).

Transgressive segregation was observed for α- and β-T percentage among NMS373 × SRA16 F_2 progeny-α- and β-T percentages ranged from 17.7 to 100.0% and 0.0 to 82.4%, respectively; 31.6% of the F_2 progeny produced less α- and more β-T than SRA16 (Fig. 1). The range of phenotypes and complexity of the phenotypic distribution were not predicted from the phenotypes of the parents or previous phenotypic analyses of the *m* or *g* mutations (Demurin 1993; Demurin et al. 1996). NMS373 × SRA16 was predicted to be segregating for the *m* locus only and, if the original hypothesis had been correct, should have segregated 3 m^+:1 *m m*. However, *m* and a second, previously unidentified locus segregated and produced four non-overlapping

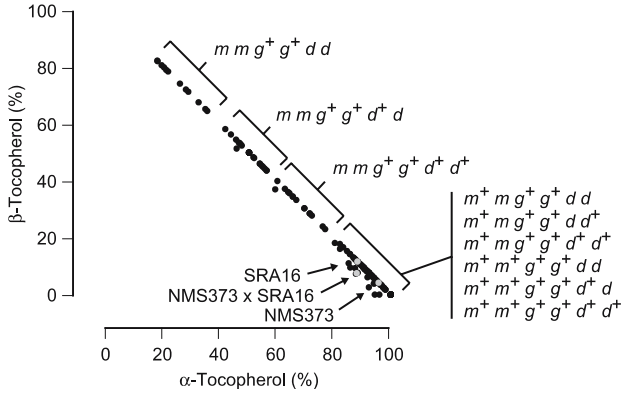

Fig. 1 Tocopherol profiles for F_2 progeny segregating for the *m* and *d* mutations. α- and β-tocopherol profiles and *m*, *g*, and *d* locus genotypes for 190 NMS373 × SRA16 F_2 progeny

phenotypic classes (Fig. 1). The origin of the mystery mutation was initially unclear and could not be ascertained from biochemical phenotypes; however, through the forward genetic analyses described here, the mutation was discovered to have been transmitted by NMS373, an inbred line with a wildtype tocopherol profile, and to be allelic to *d* mutations identified in segregating populations developed for mapping the *g* locus (Hass et al. 2006). Thus, the genotype for NMS373 was inferred to be m^+ m^+ g^+ g^+ *d d*, not m^+ m^+ g^+ g^+ d^+ d^+ as originally predicted from the wildtype tocopherol profile (Fig. 1).

The observed segregation ratio in the NMS373 × SRA16 F_2 population (139 m^+ _ _ _ : 12 *m m* d^+ d^+ : 24 *m m* d^+ *d* : 15 *m m d d*) was not significantly different from 12 m^+ _ _ _ : 1 *m m* d^+ d^+ : 2 *m m* d^+ *d* : 1 *m m d d* ($\chi^2 = 0.91$; $P = 0.82$), and was predicted to have been caused by the segregation of epistatically interacting recessive and codominant mutations (*m* and *d*, respectively). The *m* locus was epistatic to the *d* locus the latter had no effect in individuals and inbred lines carrying wildtype *m* alleles (m^+). NMS373 × SRA16 F_2 progeny producing ≥ 80.3% α-T were inferred to be m^+ m^+ or m^+ *m*, whereas progeny producing ≤ 76.9% α-T were inferred to be *m m* (the *m* allele was recessive to the m^+ allele). The observed segregation ratio for the *m* locus (139 m^+_ : 51 *m m*) was not significantly different from 3 m^+ _ : 1 *m m* ($\chi^2 = 0.34$; $P = 0.56$). The phenotypic effects of the *d* locus were imperceptible among m^+ m$^+$ and m^+ *m* individuals, but significant and additive among *m m* individuals (Fig. 1). The *d* locus genotypes of *m m* individuals producing ≤ 35.3, 41.7 to 56.3, and 59.3 to 76.9% α-T were inferred to be *d d*, d^+ *d*, and d^+ d^+, respectively (the *d* and d^+ alleles were codominant). The observed segregation ratio for the *d* locus among *m m* individuals (12 d^+ d^+ : 24 d^+ *d* : 15 *d d*) was not significantly different from 1 d^+ d^+ : 2 d^+ *d* : 1 *d d* ($\chi^2 = 0.53$; $P = 0.77$).

Genetic mapping of the *m* locus

Bulk segregant analyses (BSA) (Michelmore et al. 1991) were performed to identify SSR markers linked to the *m* locus. We screened 95 previously mapped and strategically located SSR marker loci, 78 from the SSR-multiplexes described by Tang et al. (2003) and another 17 in intervals not covered by the latter. m^+ m^+ and *m m* DNA bulks were produced using 10 individuals selected from the upper and lower tails of the NMS373 × SRA16 α-T distribution (Fig. 1). F_2 progeny producing 100% α-T were deduced to be wildtype homozygotes (m^+ m^+), whereas F_2 progeny producing ≤ 23.1% α-T were deduced to be mutant homozygotes

(*m m*). Of the 95 SSR markers screened for polymorphisms, 28 were polymorphic between the parents and two of the 28 (ORS610 and ORS716) were polymorphic between m^+ m^+ and *m m* DNA bulks. ORS610 and ORS716 previously mapped to the upper end of linkage group 1 (LG 1) (Tang et al. 2002, 2003; Yu et al. 2003). We screened 23 SSR markers proximal to ORS610 and ORS716 on LG 1 and identified four additional polymorphic SSR markers between both the parents and DNA bulks (ORS822, ORS1285, ORS605, and ORS965). The six polymorphic SSR markers from LG 1 were genotyped in NMS373 × SRA16 and assembled into a group with an order identical to previously reported orders (Tang et al. 2002; Yu et al. 2003). The *m* locus mapped to LG 1 and cosegregated with ORS605 and ORS610 (Fig. 2).

The isolation and development of single-, double-, and triple-mutant inbred lines

SRA16 is one of several offtype inbred lines we developed through phenotypic selection in R112 × LG24 or crosses between NMS373 and selected R112 × LG24 individuals; inbred lines were developed for six of eight

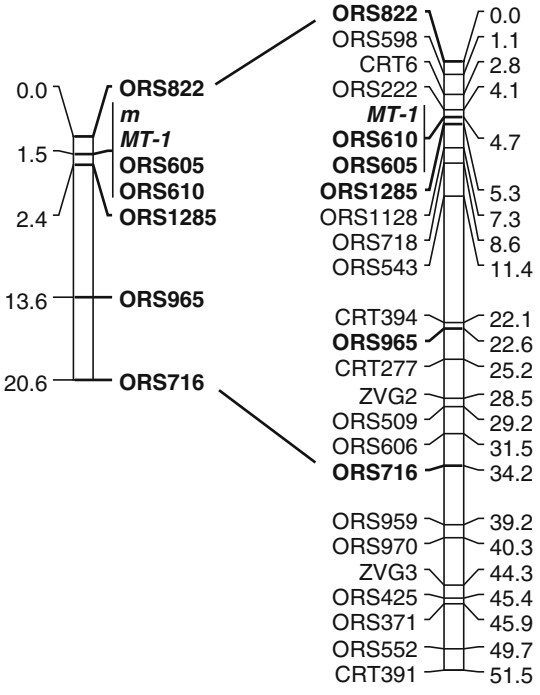

Fig. 2 Genetic mapping of *MPBQ/MSBQ-MT* and tocopherol mutant loci. Genetic mapping of *m* and *MT-1* in the NMS373 × SRA16 F_2 (displayed on the left) and *MT-1* in the RHA280 × RHA801 recombinant inbred line (displayed on the right) mapping populations. SSR marker loci (ORS and CRT prefixes) genotyped in both mapping populations are highlighted in *bold*

m × *g* × *d* locus homozygotes (m^+ m^+ g^+ g^+ d^+ d^+ and m^+ m^+ *g g d d* inbred lines were not isolated) (Table 1). R112 × LG24 was homozygous for the *m* mutation and segregating for *g* and *d* mutations (Hass et al. 2006). We developed inbred lines for each of the homozygotes produced by the segregation of *g* and *d* in R112 × LG24 by phenotyping half-seed samples, selecting F_2 individuals from the tails of the *m m* g^+_ d^+_, *m m g g* d^+_, *m m* g^+_*d d*, and *m m g g d d* distributions, selecting within F_3 and F_4 lines, and advancing selected individuals by single-seed-descent (SSD) (Table 1). The inbred lines developed from R112 × LG24 were SRA16 (*m m* g^+ g^+ d^+ d^+), HG81 (*m m g g* d^+ d^+), MB17 (*m m* g^+ g^+ *d d*), and HD55 (*m m g g d d*) (Table 1). MB17 and HG81 F_5 were isolated by selecting F_2 individuals with parental phenotypes (F_2-17 and 81, respectively) and had seed tocopherol profiles close to the parents (R112 and LG24, respectively). SRA16 and HD55 F_5 were isolated by selecting F_2 individuals with non-parental phenotypes (F_2-16 and 55, respectively) and had seed tocopherol profiles different from the parents. SRA16 produced slightly less α-T than wildtype inbred lines, whereas HD55 produced significantly more δ-T than previously described mutant inbred lines (Demurin 1993; Demurin et al. 1996).

VHG8 F_3 was developed by selecting an individual (F_2-8) from the upper tail of the γ-T distribution among F_2 progeny from a cross between NMS373 (m^+ m^+ g^+ g^+ *d d*) and R112 × LG24 F_2-81 (*m m g g* d^+ d^+). VHG8 is homozygous for the *g* mutation only (m^+ m^+ *g g* d^+ d^+) and produced 95.2% γ-T (Table 1). VHB18 and VHB45 F_3 were developed by selecting and selfing two individuals (F_2-18 and 45) from the upper tail of the β-T distribution among F_2 progeny from a cross between NMS373 and R112 × LG24 F_2-17 (*m m* g^+ g^+ *d d*). VHB18 and VHB45 are homozygous for *m* and *d* mutations (*m m* g^+ g^+ *d d*) and produced 69.7 and 74.1% β-T, respectively (Table 1).

Identification and isolation of *MPBQ/MSBQ-MT* paralogs

We identified and isolated full-length cDNA and genomic DNA sequences for two *MPBQ/MSBQ-MT* paralogs (*MT-1* and *MT-2*) and resequenced *MT-1* and *MT-2* alleles from NMS373 (*d d*), R112 (*m m d d*), LG24 (*m m g g*), and the wildtype parents of the RHA280 × RHA801 recombinant inbred line (RIL) mapping population (Supplemental Figs S1, S2; GenBank Acc. No. DQ229835-39 for *MT-1* and DQ229840-44 for *MT-2*). BLAST searches of the Compositae Genome Program Database (CGPdb; http://cgpdb.

ucdavis.edu/) and GenBank (http://www.ncbi.nlm.nih.gov/) identified several sunflower ESTs with significant homology to Arabidopsis *MPBQ/MSBQ-MT* (GenBank Acc. No. AB0542571 and At3g63410; Cheng et al. 2003; Motohashi et al. 2003). The ESTs assembled into two contigs: *MT-1* (QH_CA_Contig1970_1, QHL18E18, and AJ318323) and *MT-2* (QH_CA_Contig5553, QH_CA_Contig1970, QHL4J09, and QHN2M13).

cDNA clones for three ESTs (QHE12G15, QHJ10M08, and QHM8H03) were isolated, sequenced, and supplied slightly longer contigs (925 bp for *MT-1* and 802 bp for *MT-2*). Full-length *MT-1* cDNA sequences were isolated from NMS373, RHA280, and RHA801 using cDNA fragments amplified from developing-seed RNAs; cDNA fragments could not be amplified from R112 (*m m d d*) and LG24 (*m m g g*) (Supplemental Fig. S1). Two *MT-1* cDNA haplotypes were identified. The cDNAs isolated from NMS373 and RHA280 (1,560 bp) were identical and longer than the RHA801 cDNA (1,454 bp); the RHA801 cDNA lacked the last 106 bp of the 3′-UTR. Full-length *MT-2* cDNA sequences were isolated from NMS373, RHA280, RHA801, R112, and LG24 using cDNA fragments amplified from developing-seed RNAs (Supplemental Fig. S2). Two *MT-2* cDNA haplotypes were identified: the cDNAs isolated from NMS373, R112, RHA280, and RHA801 were identical (1,328 bp) and longer than the LG24 cDNA (1,298 bp).

MT-1 and *MT-2* coding sequences (1,017 and 1,029 bp, respectively) and chloroplast transit peptides (162 and 174 bp, respectively) were identified, translated, and aligned with Arabidopsis and other plant *MPBQ/MSBQ-MT* amino acid sequences (Supplemental Fig. S3). *MT-1* and *MT-2* encode 339 and 343 amino acids, respectively. The amino acid similarity between *MT-1* and *MT-2* was 88% (the nucleotide identity between *MT-1* and *MT-2* cDNAs was 81%). Three conserved motifs (SAM I, II, and III) characteristic of *S*-adenosyl methionine-dependent methyltransferases (Kagan and Clarke 1994; Joshi and Chiang 1998) were identified in *MT-1* and *MT-2*. The amino acids sequences for SAM I (VVDVGGGTGF) and SAM II (IEGDAEDLPF), binding sites for substrate *S*-adenosyl methionine, were identical in *MT-1* and *MT-2*. The amino acid sequences for SAM III ([L/I]K[I/K]GGKAC[V/L]), the binding site for catalytic products, were 67% similar between *MT-1* and *MT-2*. The chloroplast transit peptides (CTPs) of *MT-1* and *MT-2* (54 and 58 AAs, respectively) were predicted using ChloroP 1.1 (http://www.cbs.dtu.dk/services/chlorop-1.1/) and found to be 37% similar.

The *m* mutation is a knockout of *MPBQ/MSBQ-MT-1* caused by the insertion of a 5.2 kb *Ty3/gypsy*-like retrotransposon in exon 1

The full-length *MT-1* and *MT-2* cDNA sequences supplied templates for isolating full-length genomic DNA sequences for *MT-1* and *MT-2* from wildtype and mutant inbred lines (Supplemental Figs S1, S2). Three exons (557, 307, and 153 bp, respectively), two introns, and variable length 5′-UTRs (265–267 bp) and 3′-UTRs (172–280 bp) were identified in an alignment of NMS373, R112, LG24, RHA280, and RHA801 allele sequences for *MT-1* (Fig. 3). Three *MT-1* haplotypes were identified and distinguished by 136 single nucleotide polymorphisms (SNPs), 26 insertion–deletion (INDEL) polymorphisms, and double-stranded DNA hairpin structures in both introns: haplotype 1 (9,460 bp) was found in R112 and LG24, haplotype 2 (3,752 bp) was found in RHA801, and haplotype 3 (4,517 bp) was found in NMS373 and RHA280 (Fig. 3; Supplemental Fig. S1). Fourteen long INDELs (51–5,175 bp) were identified among the three haplotypes. Three non-synonymous SNPs were identified in *MT-1* coding sequences (CDSs)—CTA (Leu-50) to CCA (Pro-50), CAG (Gln-252) to AAG (Lys-252), and CTT (Leu-311) to GTT (Val-311)—but none were associated with phenotypes produced by *m* or *d*, e.g., the Leu-50 SNP allele was found in m^+ m^+ (NMS373; haplotype 3) and *m m* (R112 and LG24; haplotype 1) and the Lys-252 SNP allele was found in d^+ d^+ (LG24) and *d d* (R112) inbred lines (Supplemental Fig. S1).

MT-1 haplotype 1 was distinguished from haplotypes 2 and 3 by the absence of a hairpin structure in intron 1, presence of a 438 bp insertion in the 3′-UTR (184 bp downstream of the stop codon), and presence of a 5,175 bp insertion in exon 1, in addition to other DNA polymorphisms (Fig. 3; Supplemental Fig. S1). The 438 bp insertion in the 3′-UTR carries a $[CCGATTTTTT]_8$ repeat; significant BLAST hits were not retrieved from GenBank when the 438-bp INDEL was used as query template. The 5,175 bp insertion was identified to be a *Ty3/gypsy*-like long-terminal-repeat (LTR) retrotransposon (Song et al. 1994; Bowen and McDonald 2001; Feschotte et al. 2002) and was predicted to knockout the *MT-1* allele found in R112, LG24, SRA16, and other inbred lines carrying the *m* mutation. The *Ty3/gypsy*-like retrotransposon inserted into the SAM I motif found in exon 1 of *MT-1* and seems to be complete—*gag* (1,401 bp) and *pol* (3,057 bp) genes were present and flanked by 5′ and 3′ tandem LTRs (234 bp) (Marchler-Bauer and Bryant 2004). The protease (PR), reverse transcriptase (RT), and intergrase (IN) domains in the *pol* gene were

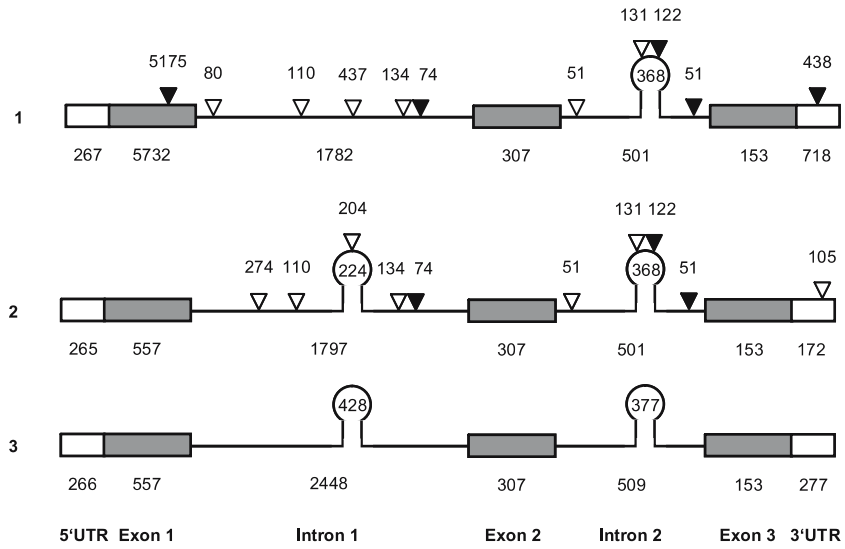

Fig. 3 *MPBQ/MSBQ-MT-1* insertions, deletions, hairpins, and haplotypes. Schematic diagram illustrating UTRs (*white boxes*), exons (*dark gray boxes*), introns (*lines*), insertions (*inverted black triangles*), deletions (*inverted white triangles*), and hairpins found in three *MPBQ/MSBQ-MT-1* haplotypes (1, 2, and 3). UTR, exon, and intron lengths (bp) are shown below each haplotype, INDEL lengths are shown above each haplotype, and hairpin lengths are shown within the bulb of each hairpin. The mutant *MT-1* allele (*m*) harbors a 5,175 bp *Ty3/gypsy*-like retrotransposon insertion in exon 1 and was found in R112 and LG24 (haplotype 1; 9,460 bp). Wildtype *MT-1* alleles (m^+) were found in RHA801 (haplotype 2; 3,752 bp) and NMS373 and RHA280 (both haplotype 3; 4,517 bp). INDEL lengths are in reference to haplotype 3

present in the order (PR-RT-IN) found in *Ty3/gypsy*-like retrotransposons; the order in *copia*-like retrotransposons is PR-IN-RT (Song et al. 1994; Bowen and McDonald 2001; Feschotte et al. 2002).

We tested for an association between *MT-1* and *m* by developing INDEL markers diagnostic for mutant and wildtype *m* alleles, screening several wildtype (m^+ m^+) and mutant (*m m*) homozygotes for presence or absence of the exon 1 and 3′-UTR insertions found in haplotype 1, screening for cosegregation between *MT-1* and *m* in the NMS373 × SRA16 F_2 population, and screening for *MT-1* transcription in wildtype (m^+ m^+) and mutant (*m m*) homozygotes. The 438-bp insertion in the 3′-UTR and 5,175-bp insertion in exon 1 of haplotype 1 were amplified from genomic DNAs of R112, LG24, and six other mutant (*m m*) homozygotes (SRA16, VHB18, VHB45, HG81, MB17, and HD55) only (Fig. 4). Neither insertion was present in wildtype (m^+ m^+) homozygotes (NMS373, VHG8, RHA280, and RHA801). RT-PCR analyses were performed on RNAs isolated from developing seeds and leaves using *MT-1* specific primers flanking intron 1 (F38/R57); the primer site DNA sequences were identical among the three haplotypes (Table 2; Supplemental Fig. S1). *MT-1* transcripts of the predicted length (320 bp) were amplified from m^+ m^+ inbred lines only (Fig. 4). No transcripts were amplified from *m m* inbred lines; hence, as predicted from R112 and LG24 allele sequences, *MT-1* was not transcribed in *m m* homozygotes and *MT-1* was knocked out by the insertion of a 5.2 kb *Ty3/gypsy*-like retrotransposon in exon 1.

DNA sequences homologous to class I and II transposons in *MT-1* and *MT-2* introns

Fourteen DNA fragments homologous to class I or II transposable elements (Bennetzen 2000; Feschotte et al. 2002; Jiang et al. 2004) were identified in the introns of *MT-1* and *MT-2* (Supplemental Figs. S1, S2). Nucleotide identities among sunflower and heterologous rice, maize, or Arabidopsis transposon sequences (Jiang et al. 2004; http://www.tigr.org/tdb/e2k1/ plant.repeats/) ranged from 54 to 58%. The first intron of *MT-1* harbored DNA sequences (identified by length) homologous to *adh*-like miniature inverted repeat transposable elements (MITEs) (247 and 243 bp), *Ty1/copia*- and *Ty3/gypsy*-like retrotransposons (364 and 426 bp), and *en/spm*-like (*CACTA*) transposons (434 bp). The second intron of *MT-1* harbored DNA sequences homologous to *activator* (*Ac*) (181-bp) and *en/spm*-like (148-bp) transposons and *tourist*-like MITEs (101-bp). The second intron of *MT-2* harbored DNA sequences

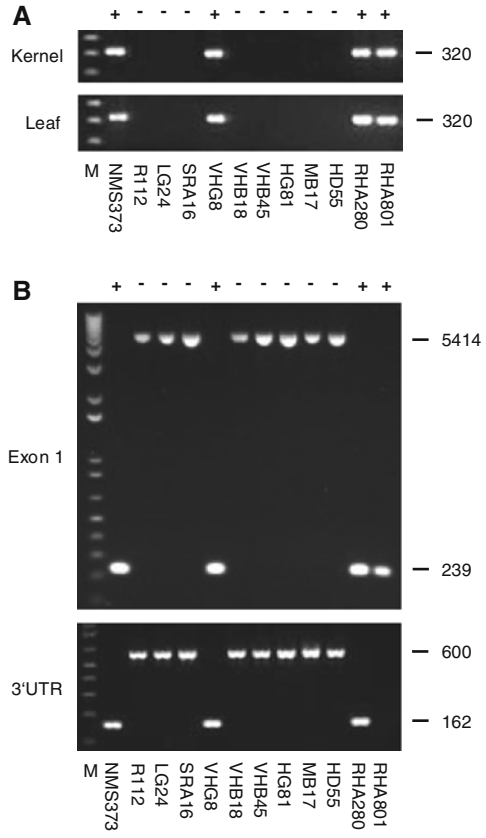

Fig. 4 *MPBQ/MSBQ-MT-1* is not transcribed in mutant homozygotes (*m m*). (**a**) Ethidium bromide-stained agarose gel showing cDNA fragments amplified by RT-PCR from RNAs isolated from developing seeds (25-DAF) and leaves (60-DAG) of four homozygous wildtype ($m^+ m^+ = +$) inbred lines (NMS373, VHG8, RHA280, and RHA801) and eight homozygous mutant (*m m* = −) inbred lines (R112, LG24, SRA16, VHB18, VHB45, HG81, MB17, and HD55) using a primer pair (F38/R57) flanking the first intron in *MT-1*. F38/R57 amplified a 320 bp cDNA fragment from wildtype (+) inbred lines only. M is a DNA ladder. **b** Ethidium bromide-stained agarose gel showing DNA fragments amplified by LD-PCR from genomic DNAs isolated from four homozygous wildtype ($m^+ m^+ = +$) inbred lines (NMS373, VHG8, RHA280, and RHA801) and eight homozygous mutant (*m m* = −) inbred lines (R112, LG24, SRA16, VHB18, VHB45, HG81, MB17, and HD55) using primer pairs in exon 1 (F8/ R39) and the 3′-UTR (F76/R83) of *MT-1*. F8/R39 amplified a 239 bp DNA fragment from wildtype (+) and 5,414 bp DNA fragment from mutant (−) inbred lines. F76/R83 amplified a 162 bp DNA fragment from three of the four wildtype (+) and a 600 bp DNA fragment from mutant (−) inbred lines. F76/R83 did not amplify a DNA fragment from RHA801 because the reverse primer is complementary to DNA sequences deleted in the RHA801 allele. M is a DNA ladder

homologous to *bg* transposons (252-bp) and *tourist*-like MITEs (230 and 249 bp). Finally, the third intron of *MT-2* harbored DNA sequences homologous to *Ac–Ds* transposons (266-bp), *adh*-like MITEs (553-bp), and *copia*-like retrotransposons (796-bp).

Codominant INDEL markers diagnostic for the *MT-1* mutation

Codominant INDEL markers diagnostic for mutant and wildtype *MT-1* alleles were developed by combining three primers in allele-specific combinations targeting DNA sequences within (R15 and F32) and upstream (F8) and downstream (R39) of the retrotransposon in exon 1 (F8/F32/R39 and F8/R15/R39) (Fig. 5; Table 2). The F8/R39 primer combination was used in both genotyping assays, flanks the retrotransposon, and is wildtype allele specific. When used in standard PCR analyses, F8/R39 amplified a 239 bp genomic DNA fragment from $m^+ m^+$ inbred lines, but failed to amplify the 5,414 bp genomic DNA fragment from *m m* inbred lines (Fig. 5). R15 and F32 are complementary to retrotransposon DNA sequences; hence, the F8/R15 and F32/ R39 primer combinations are mutant allele specific. When standard PCR analyses were performed using the F8/F32/R39 primer combination, the F8/R39 primer pair amplified a 239 bp DNA fragment from $m^+ m^+$ inbred lines, whereas the F32/ R39 primer pair amplified a 339 bp DNA fragment from *m m* inbred lines. Similarly, when standard PCR analyses were performed using the F8/R15/R39 primer combination, the F8/R39 primer pair amplified a 239 bp DNA fragment from $m^+ m^+$ inbred lines, whereas the F8/R15 primer pair amplified a 329 bp DNA fragment from *m m* inbred lines. We developed a third codominant INDEL marker for *MT-1* by targeting primers (F45/R50) to DNA sequences flanking INDEL polymorphisms found in intron 1, primarily for mapping the *MT-1* locus in reference populations segregating for different wildtype alleles (e.g., RHA280 × RHA801) (Table 2). The F45/R50 INDEL marker amplified alleles of the predicted length from mutant and wildtype inbred lines. The *MT-1* locus was genotyped in the RHA280 × RHA801 RIL population ($n = 94$) using the F45/F50 INDEL marker and in the NMS373 × SRA16 F_2 population ($n = 190$) using two INDEL markers (F8/F32/R39 and F45/50), mapped to linkage group 1, and cosegregated with the *m* locus (Figs. 2, 6).

MPBQ/MSBQ-MT-2 transcription was twofold greater in developing seeds of wildtype ($d^+ d^+$) than mutant (*d d*) inbred lines

Once associations between *MT-1* and *m* and *γ-TMT* and *g* were discovered and *MT-1*, *γ-TMT*, and *TC* loci were found to segregate independently of the *d* locus (Fig. 2; Hass et al. 2006), our search for the function disrupted by the *d* mutation narrowed to *MT-2*. We

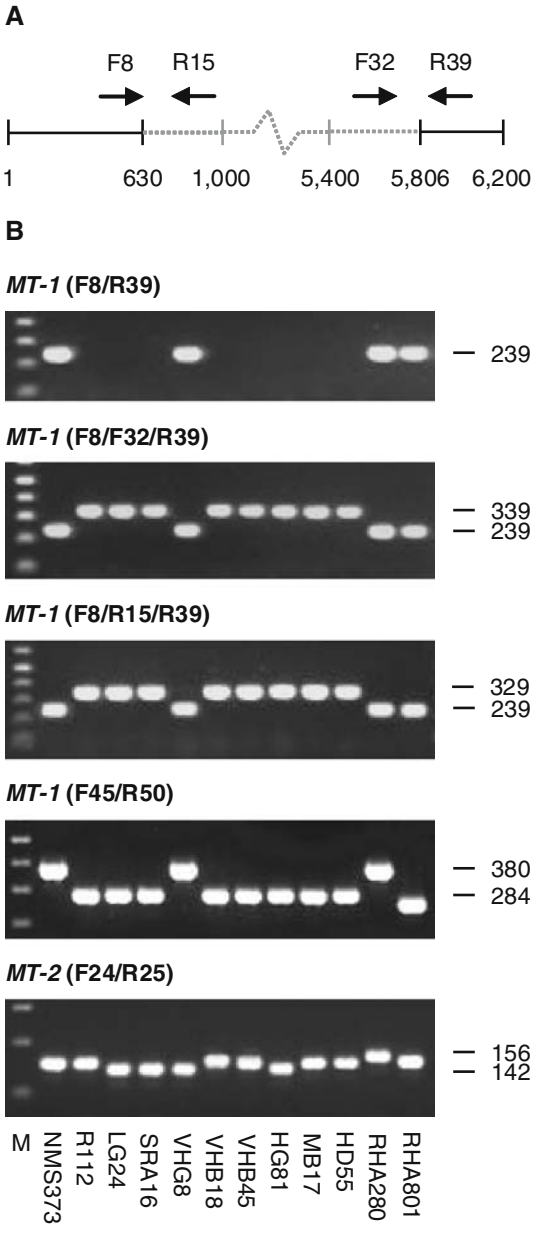

Fig. 5 *MT-1* and *MT-2* INDEL marker polymorphisms. **a** Locations (nt) for forward (F8 and F32) and reverse (R15 and R39) oligonucleotide primers for INDEL markers diagnostic for presence or absence of the *Ty3/gypsy*-like retrotransposon insertion (*dotted line*) in exon 1 (*solid line*) of *MT-1*. **b** Length polymorphisms (bp) for *MT-1* and *MT-2* insertion–deletion (INDEL) markers among several inbred lines (ethidium bromide-stained agarose gels showing genomic DNA fragments amplified by PCR using *MT-1* or *MT-2* specific oligonucleotide primers). The F8/R39 primer pair flanks the 5,175-bp *Ty3/gypsy*-like retrotransposon insertion in exon 1 of *MT-1* and, when standard PCR protocols are used, does not amplify genomic DNA fragments from mutant homozygotes (*m m*). The F8/F32/R39 and F8/R15/R39 primer combinations are allele specific and amplify wildtype and mutant *MT-1* alleles. F8/R39 amplified a 239 bp allele from wildtype homozygotes (m^+ m^+), whereas F32/R39 amplified a 339 bp allele from mutant homozygotes (*m m*). F8/R39 amplified a 239 bp allele from wildtype homozygotes (m^+ m^+), whereas F8/R15 amplified a 329 bp allele from mutant homozygotes (*m m*). The F45/R50 *MT-1* INDEL marker targets INDELs in the first intron. The F24/R25 *MT-2* INDEL marker targets INDELs in the third intron. M is a DNA ladder

isolated and aligned full-length genomic DNA sequences from mutant (*d d*) and wildtype (d^+ d^+) inbred lines and searched for non-synonymous SNPs and other DNA polymorphisms. Three *MT-2* haplotypes were identified and shared 33 SNPs and 11 INDELs: haplotype 1 (3,768 bp) was found in NMS373, R112, and RHA801, haplotype 2 (3,312 bp) was found in LG24, and haplotype 3 (3,780 bp) was found in RHA280 (Supplemental Fig. S2). Eight SNPs were identified in *MT-2* CDSs, but none were non-synonymous. Several SNPs and INDELs were found in introns 2 and 3. Other than a 12 bp INDEL in intron 3, the SNP and INDEL alleles found in haplotypes 1 and 3 were identical (LG24 carried the opposite SNP or INDEL allele). We found a 361 bp hairpin structure in intron 2 of haplotypes 1 and 3. The hairpin structure was deleted in haplotype 2 and spanned a 372 bp INDEL. Haplotypes 1 and 3 carried a 30 bp insertion at the beginning of the 5′-UTR (deleted in haplotype 2). Thus, several SNPs and INDELs distinguish the *MT-2* allele found in LG24 and SRA16 (d^+ d^+) from the *MT-2* allele found in R112 and NMS373 (*d d*); the d^+ allele found in SRA16 was transmitted by LG24 (Hass et al. 2006).

The presence of the 30 bp INDEL at the beginning of the 5′-UTR was substantiated by using 5′-RACE PCR to amplify cDNA fragments from developing seed RNAs isolated from R112, NMS373, and LG24 (data not shown). We developed RT-PCR and genotyping assays to screen for the INDEL by targeting a forward primer (F1) to the inserted DNA sequence and a reverse primer (R7) to shared DNA sequences downstream of the insertion site (Fig. 7; Table 2). F1/R7 amplified *MT-2* transcripts (306 bp) and genomic DNA fragments (582 bp) from *d d* (mutant) inbred lines only. We developed a second RT-PCR and genotyping assay for *MT-2* by positioning a forward primer (F5) upstream and reverse primer (R7) downstream of intron 1 (Table 2). F5/R7 amplified *MT-2* transcripts (209 bp) and genomic DNA fragments (485 bp) from mutant and wildtype inbred lines; hence, *MT-2* was transcribed in d^+ d^+ and *d d* inbred lines (Fig 7).

Table 2 *MPBQ/MSBQ-MT-1* and *MT-2* Primer Sequences

Gene	Name	Location (nt)[a]	Orientation[b]	Sequence (5′–3′)
MT-1	F8	427	F	AGATGTAGTGTGTCTGTATCA
MT-1	R15	755	R	GGTTTACAACGACTACAACTA
MT-1	F32	5,502	F	GTCTCCAGCTTCGTTTTCCAT
MT-1	F38	5,819	F	CTACTTTGGGGATTGTGGAACA
MT-1	R39	5,840	R	TGTTCCACAATCCCCAAAGTAG
MT-1	F45	7,209	F	AGAGAAGAACGTAATGCTAGG
MT-1	R50	7,604	R	TGGTAAGCAAATGGGACAAGA
MT-1	R57	8,688	R	CAACATCCACATGTCTGCAAAG
MT-1	F76	9,737	F	AGCTTGTGTGCACTGTTATTTG
MT-1	R83	10,336	R	TACGAAGCTACATAACCACTTG
MT-2	F1	1	F	GATTATCAACAGCCGTATACTTGG
MT-2	F5	98	F	TCAATGGTGCTTTGAGTCAAC
MT-2	R7	582	R	ACACTTAGGTACAACTAAGGT
MT-2	F10	872	F	CGAAGCAAAAGGAACCGTTGAA
MT-2	R14	1,827	R	ATCTTTAGAACTCGATATGCCT
MT-2	F24	2,913	F	CTACTTACCTGTTGATAAACC
MT-2	R25	3,080	R	GTTATATCGGTCAATATCGCCA

[a] Nucleotide locations in genomic DNA sequence alignments for *MT-1* and *MT-2* (Supplemental Figs. S1, S2)

[b] Forward (F) and reverse (R)

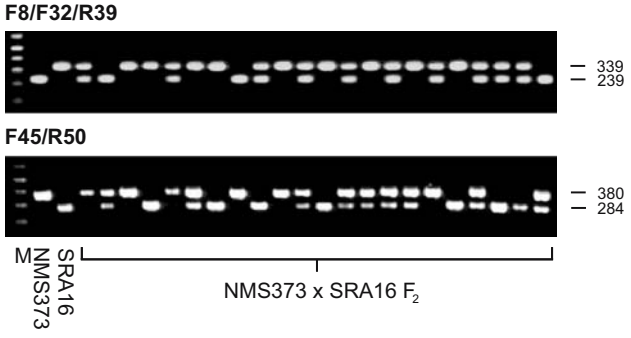

Fig. 6 *MT-1* INDEL marker genotyping in the NMS373 × SRA16 F_2 mapping population. F8/F32/R39 and F45/R50 *MT-1* INDEL marker genotypes among 22 NMS373 × SRA16 F_2 progeny. M is a DNA ladder

Codominant INDEL markers diagnostic for the *MT-2* mutation

We developed an INDEL marker (F24/R25) diagnostic for *MT-2* haplotypes by positioning a forward primer (F24) upstream and reverse primer (R25) downstream of an INDEL in intron 3; 12 bp (nt 3,009–3,035) were deleted in haplotype 1 and 26 bp (nt 3,036–3,047) were deleted in haplotype 2 (Fig. 5; Table 2). The *MT-2* locus was genotyped in the NMS373 × SRA16 F_2 mapping population using the F24/F25 INDEL marker and cosegregated with the *d* locus. The only putative mutation we found between wildtype and mutant *MT-2* alleles was the 30 bp insertion at the beginning of the 5′-UTR in the R112 and NMS373 alleles. The insertion was predicted to affect *MT-2* transcription. We developed a quantitative RT-PCR assay for *MT-2* and screened LG24 and HG81 (d^+ d^+) and NMS373 and R112 (*d d*) for *MT-2* transcript accumulation differences in leaves and developing seeds (Fig. 7); LG24 is the source of the wildtype *d* allele found in HG81 (Hass et al. 2006). The forward (F10) and reverse (R14) primers used in the RT-PCR assay targeted DNA sequences in exons 1 and 2, respectively (Table 2). *MT-2* transcription was identical in R112 and NMS373 (*d d* inbred lines), 2.2 to 2.3-fold greater in leaves of d^+ d^+ than *d d* inbred lines, and 3.4 to 5.0-fold greater in developing seeds of d^+ d^+ than *d d* inbred lines (Fig. 7).

Intragenic and intergenic effects of *MT-1* and *MT-2*

The development of INDEL markers diagnostic for mutant and wildtype *MT-1* and *MT-2* alleles supplied the tools needed to identify *MT-1* and *MT-2* locus genotypes underlying tocopherol phenotypes, estimate the intragenic and intergenic effects of *MT-1* and *MT-2*, and estimate *MT-1* × *MT-2* genotype means (Tables 3, 4). Segregation ratios for *MT-1* (52:88:50; $\chi^2 = 1.07$; $P = 0.58$) and *MT-2* (41:101:48; $\chi^2 = 1.27$; $P = 0.53$) INDEL marker loci were not significantly different from 1:2:1 (neither locus had distorted segregation ratios). *MT-1* and *MT-2* significantly decreased α- and increased β-T percentages and epistatically interacted ($P < 0.0001$ for α- and β-T percentage) (Tables 3, 4). Neither locus significantly affected γ- or δ-T percentages (statistics not shown). The additive effects of *MT-1* were fourfold greater than the additive effects of *MT-2* and were of opposite sign because the mutant alleles were transmitted by different parents (*m* by SRA16 and *d* by NMS373). The intra- and intergenic effects of the two loci were associated with 89.0 to

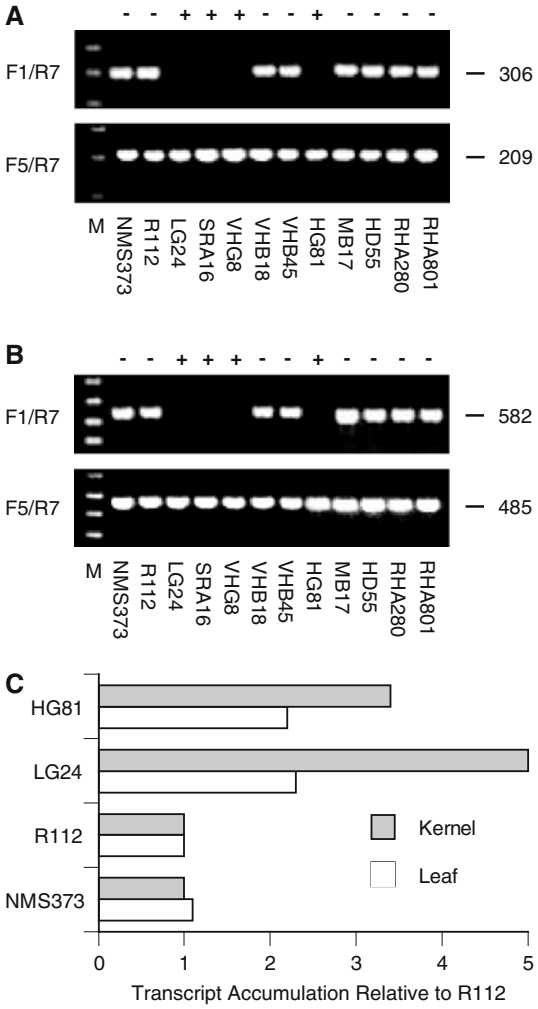

Fig. 7 *MPBQ/MSBQ-MT-2* is more strongly transcribed in wildtype (d^+ d^+) than mutant (d d) homozygotes. (**a**) Ethidium bromide-stained agarose gels showing cDNA fragments amplified by RT-PCR from RNAs isolated from developing seeds (25-DAF) of wildtype (d^+ d^+ = +) and mutant (d d = −) inbred lines using primer pairs (F1/R7 and F5/R7) flanking intron 1. The *MT-2* allele found in mutant inbred lines carries a 30 bp insertion at the beginning of the 5′-UTR. F1 is complementary to DNA sequences found in the 30-bp insertion (nt 1–24), whereas F5 is complementary to DNA sequences 30 bp downstream of the 30-bp insertion in the 5′-UTR (nt 98–119). The reverse primer (R7) is complementary to DNA sequences in exon 2 (nt 561–582). M is a DNA ladder. (**b**) Ethidium bromide-stained agarose gels showing genomic DNA fragments amplified from wildtype (d^+ d^+ = +) and mutant (d d = −) inbred lines using primers (F1/R7 or F5/R7) flanking intron 1 in *MT-2*. (**c**) *MT-2* transcript accumulation in developing seeds (25-DAF) and leaves (60-DAG) of wildtype and mutant inbred lines quantified by real-time RT-PCR using forward and reverse primers (F10/R14) flanking 163-bp in exon 1. The dependent variable (*x*-axis) was calculated using the ratio of the cycle threshold for each inbred line to the cycle threshold for R112 normalized to actin (*x* = 1 for R112)

90.0% of the phenotypic variability observed among NMS373 × SRA16 F_2 progeny (Table 4). *MT-1* was epistatic to *MT-2*⁻*MT-2* significantly decreased α- and

Table 3 *MT-1* × *MT-2* INDEL marker genotype means among 190 NMS373 × SRA16 F_2 progeny

Genotype[a]		Tocopherol (%)			
MT-1 × *MT-2*	*m* × *g* × *d*	α	β	γ	δ
11/11	m^+ m^+ g^+ g^+ *d d*	96.7	3.1	0.1	0.2
11/12	m^+ m^+ g^+ g^+ d^+ *d*	96.1	3.5	0.3	0.1
11/22	m^+ m^+ g^+ g^+ d^+ d^+	97.5	1.8	0.2	0.6
12/11	m^+ *m* g^+ g^+ *d d*	89.1	10.7	0.2	0.0
12/12	m^+ *m* g^+ g^+ d^+ *d*	91.3	8.4	0.2	0.1
12/22	m^+ *m* g^+ g^+ d^+ d^+	92.8	7.0	0.2	0.0
22/11	*m m* g^+ g^+ *d d*	29.5	70.5	0.0	0.0
22/12	*m m* g^+ g^+ d^+ *d*	48.6	51.3	0.0	0.1
22/22	*m m* g^+ g^+ d^+ d^+	62.3	37.5	0.0	0.5

[a] INDEL marker alleles for *MT-1* and *MT-2* transmitted by NMS373 were coded 1, whereas INDEL marker alleles for *MT-1* and *MT-2* transmitted by SRA16 were coded 2; hence, *MT-1* × *MT-2* genotypes for the parents were 11/11 (NMS373) and 22/22 (SRA16), respectively. NMS373 transmitted wildtype *m* and *g* alleles and mutant *d* alleles (m^+, g^+, and *d*, respectively), whereas SRA16 transmitted mutant *m* and wildtype *g* and *d* alleles (*m*, g^+, and d^+, respectively)

increased β-T percentages among F_2 individuals homozygous for the mutant *MT-1* allele (*m m*), but had no effect among F_2 individuals heterozygous or homozygous for wildtype *MT-1* alleles (m^+ m^+ and m^+ *m*). The additive effects of *MT-2*, when estimated among mutant *MT-1* (*m m*) individuals, were −19.9% for α-T ($P < 0.0001$) and 20.0% for β-T ($P < 0.0001$). The degree of dominance of *MT-1* was incomplete (0.77 for α- and 0.76 for β-T), but sufficient to produce a discontinuous array of α- × β-T phenotypes among heterozygotes (m^+ *m*) and wildtype homozygotes (m^+ m^+) (Tables 3, 4; Fig. 1). The degree of dominance of *MT-2* was nearly completely additive (0.11 for α- and β-T).

Discussion

The tocopherol composition variability found in seeds (Cook and Miles 1992; Sheppard et al. 1993; Demurin et al. 1996; Kamal-Eldin and Andersson 1997; Dolde et al. 1999; Grusak and DellaPenna 1999; Rocheford et al. 2002; Wong et al. 2003) is primarily caused by genotypic variability among γ-*TMT* and *MPBQ/MSBQ-MT* loci (Shintani and DellaPenna 1998; Shintani et al. 2002; Bergmüller et al. 2003; Cheng et al. 2003; Van Eenennaam et al. 2003). Wildtype γ-*TMT* and *MPBQ/MSBQ-MT* activities in developing seeds of sunflower drive tocopherol synthesis towards α-T. The unparalleled diversity of wildtype and offtype tocopherol composition phenotypes found in sunflower is caused by the apparently strong γ-TMT and MPBQ/MSBQ-MT activities in developing seeds leading to

Table 4 Intragenic and intergenic effects of *MT-1* and *MT-2* on sunflower seed tocopherol profiles. Coefficients of determination (R^2) for the intragenic and intergenic effects of *MT-1* and *MT-2* (eight degrees of freedom), degree of dominance (|D/A|) of *MT-1* and *MT-2*, and statistical significance (*Pr* > F) of additive (A), dominance (D), A × A, A × D, D × A, and D × D effects of *MT-1* and *MT-2* on tocopherol percentages in seeds of 190 NMS373 × SRA16 F_2 progeny

Tocopherol Source	*MT-1A*		*MT-1D*		*MT-2A*		*MT-2D*		*MT-1 A × MT−2 A*		*MT-1 A × MT−2 D*		*MT-1 D × MT−2 A*		*MT-1 D × MT−2 D*		|D/A|	
	Effect (%)	Pr > F	Effect (%)	Pr > F	Effect (%)	Pr > F	Effect (%)	Pr > F	Effect (%)	Pr > F	Effect (%)	Pr > F	Effect (%)	Pr > F	Effect (%)	Pr > F	*MT-1*	*MT-2* R^2
α	25.0	< 0.0001	−19.3	< 0.0001	−6.2	< 0.0001	−0.7	0.54	8.0	< 0.0001	1.9	0.20	−6.5	< 0.0001	−0.6	0.79	0.77	0.11	0.89
β	−25.2	< 0.0001	19.2	< 0.0001	6.3	< 0.0001	0.7	0.52	−7.9	< 0.0001	−1.9	0.18	6.7	< 0.0001	0.4	0.86	0.76	0.11	0.90

> 90% α-T in wildtypes, mutations affecting γ-TMT and MPBQ/MSBQ-MT activities upstream of α- and β-T (the terminal products of the pathway), the multifunctionality and redundancy of *MPBQ/MSBQ-MT* loci, and epistatic interactions among γ-*TMT* and *MPBQ/ MSBQ-MT* loci (Tables 1, 3, 4; Hass et al. 2006).

Using genomic approaches and forward genetic analyses, we isolated genes encoding methyltransferases (*MT-1*, *MT-2*, γ-*TMT-1*, and γ-*TMT-2*) necessary for the synthesis of tocopherols in sunflower and identified *MPBQ/MSBQ-MT* and γ-*TMT* mutations underlying tocopherol composition phenotypes produced by four epistatically interacting loci (*MT-1*, *MT-2*, γ-*TMT-1*, and γ-*TMT-2*); γ-*TMT* paralogs were found in RHA801 and LG24, but were not found in several wildtype inbred lines (Tables 1, 3, 4; Hass et al. 2006). The independence of *m*, *g*, and *d* and associations between *MT-1* and *m*, *MT-2* and *d*, and γ-*TMT-1*, γ-*TMT-2*, and *g* were substantiated in the present and a companion study by allele resequencing, transcript profiling, and genetic mapping (Hass et al. 2003, 2006; Tang et al. 2005; Fig. 2). Our analyses focused on the $m = Tph_1$ and $g = Tph_2$ mutations identified by Demurin (1993) and *d* mutation identified by Hass et al. (2006) and supply molecular tools for rapidly identifying new methyltransferase and cyclase mutations. Several additional mutant inbred lines (T589, T2100, IAST-1, IAST-4, IAST-5, and IAST-540) have been described (Demurin et al. 2004; Velasco et al. 2004a, b), have biochemical phenotypes virtually identical to the mutant inbred lines we screened (Demurin 1993; Demurin et al. 1996; Hass et al. 2006; Table 1), and are predicted to carry novel γ-*TMT*, *MT-1*, or *MT-2* mutations.

Transposable element-induced mutations, other than the *Ty3/gypsy*-like retrotransposon knockout of *MT-1*, have not been identified in sunflower, but are common in other plant genera (Johns et al. 1985; Grandbastein et al. 1989; Varagona et al. 1992; Weil et al. 1992; Purugganan and Wessler 1994) and could be common in sunflower. *Ty1/copia*- and *Ty3/gypsy*-like retrotransposons (class I transposable elements) are found in sunflower (Santini et al. 2002), have undoubtedly played a central role in enlarging and reshaping the sunflower genome, as they have in monocots (SanMiguel et al. 1996, 1998; Bennetzen 2000, 2002; Ma et al. 2004; Lal and Hannah 2005), and have apparently proliferated at different rates among progenitor and homoploid hybrid sunflower species (Baack et al. 2005).

We identified several DNA fragments (101–796 bp in length) in *MT-1*, *MT-2*, γ-*TMT*, and *TC* introns

(Supplemental Fig. S1, S2; Hass et al. 2006) homologous to class I and II transposable elements identified in corn, rice, and Arabidopsis (Jiang et al. 2004; http://www.tigr.org/tdb/e2k1/plant.repeats/); specifically, miniature inverted repeat transposable elements (e.g., *tourist*- and *adh*-like MITEs), DNA-mediated transposons (e.g., *Ac–Ds* and *en/spm*), and RNA-mediated transposons (e.g., *Ty3/gypsy*- and *Ty1/copia*-like). Transposons typically cause mutations through intronic insertions that decrease transcription, yield multiple transcripts through alternative splicing, or activate or suppress transcription initiation sites (Varagona et al. 1992; Weil et al. 1992; Brown 1996; Lal et al. 1999, 2003; Marillonnet and Wessler 1997; Cui et al. 2003). The LTR-retrotransposons found in spontaneously induced mutant alleles are usually present in low to medium copy number (1–50) in the host genome (Purugganan and Wessler 1994; Marillonnet and Wessler 1998; Feschotte et al. 2002), in contrast to the LTR-retrotransposons found in very high copy numbers that constitute the bulk of rice, corn, and other large plant genomes (SanMiguel et al. 1996; Feschotte et al. 2002; Ma et al. 2004). The copy number of the *Ty3/gypsy*-like retrotransposon found in the mutant *MT-1* allele is not known. Unlike DNA-mediated transposons (e.g., *Ac–Ds*), most LTR-retrotransposons are inactive (Johns et al. 1985; Grandbastein et al. 1989; Varagona et al. 1992; Weil et al. 1992; Feschotte et al. 2002), and tend to induce stable mutations when active. The DNA sequences of the LTRs (234 bp) found in the *MT-1* retrotransposon were 100% identical (Supplemental Fig. S1) and suggest recent transposition (SanMiguel et al. 1998; Ma et al. 2004). The retrotransposon harbored the complete set of elements needed for autonomous transposition (Purugganan and Wessler 1994; Song et al. 1994; Bowen and McDonald 2001; Feschotte et al. 2002) and thus has the potential to be reactivated by biotic and abiotic stresses (Grandbastein 1998), as has been reported for spontaneous mutations induced by *Ty3/gypsy*- and *Ty1/copia*-like retrotransposons in other genera (Johns et al. 1985; Grandbastein et al. 1989; Purugganan and Wessler 1994).

The null *MT-1* (*m*) and near-null γ-*TMT* (*g*) alleles we identified originated in LG15 and LG17 and seem to have arisen spontaneously in open-pollinated populations (VMIIK8931 and VIR44, respectively; Demurin 1993; Demurin et al. 1996). The cryptic partial loss-of-function *MT-2* alleles (*d*) we uncovered in B109 × LG24, R112 × LG24, and NMS373 × SRA16 spontaneously arose, but were masked by wildtype *MT-1* and γ-*TMT* alleles found in wildtype inbred lines (Fig. 1; Table 1; Hass et al. 2006). T589 and T2100 carry spontaneous mutations found in open-pollinated populations, PI 307937 and CO-77-256, respectively (Velasco et al. 2004a). The biochemical phenotypes for T589 and T2100 were virtually identical to LG15 (*m m*) and LG17 (*g g*); hence, T589 and T2100 probably carry loss-of-function *MT-1* and γ-*TMT* mutations, respectively. The mutant alleles found in IAST-1, IAST-4, IAST-5, and IAST-540 were induced using ethylmethane sulfonate (EMS) (Velasco et al. 2004b) and could harbor G/C-to-A/T or other single nucleotide transitions leading to non-synonymous amino acid substitutions in γ-*TMT*, *MT-1*, *MT-2*, and *TC* (Hoffmann 1980; Greene et al. 2003). The spontaneous and induced mutations carried by T- and IAST-series inbred lines (Velasco et al. 2004a, b) can be rapidly identified by resequencing γ-*TMT*, *TC*, *MT-1*, or *MT-2* alleles and screening for non-synonymous SNPs and other DNA polymorphisms using the genomic DNA sequences and locus-specific primers described herein (Table 2; Supplemental Fig. S1, S2; Hass et al. 2006).

The discovery of genetic mechanisms and cDNA and DNA polymorphisms underlying the *m*, *g*, and *d* mutations and development of single, double, and triple mutant inbred lines (Figs. 1, 2; Tables 1, 2, 3 and 5, 6; Hass et al. 2006) facilitated the development of models for understanding and predicting tocopherol composition phenotypes and unravelling the often complex phenotypic effects produced by the duplicated, epistatically interacting methyltransferase loci found in sunflower. Hass et al. (2006) observed a decrease in α-T among R112 × LG24 F_2 individuals homozygous for the *MT-1* knockout mutation (*m*)—*m m* g^+ g^+ d^+ d^+ genotypes produced 86.2% α-T and 13.8% β-T. The *m m* g^+ g^+ d^+ d^+ inbred line (SRA16) we isolated from R112 × LG24 produced 88.5% α-T and 8.8% β-T (Table 1). The decrease in α-T and increase in β-T percentage were consistent with partially diminished MPBQ/MSBQ-MT activity and increased flow through the MPBQ ⇒ δ-T ⇒ β-T branch of the pathway (Cheng et al. 2003; Van Eenennaam et al. 2003). *MT-2* activity seems to have nearly completely compensated for the loss of *MT-1* activity in *m m* g^+ g^+ d^+ d^+ genotypes because flow through the MPBQ ⇒ DMPBQ ⇒ γ-T ⇒ α-T branch of the pathway was only slightly diminished.

The *d* alleles we identified produced quantitative effects and may have been segregating in one or more of the populations phenotyped by Demurin et al. (1996) and Velasco et al. (2004a, b). The development and genetic mapping of *MT-2* DNA markers should facilitate the identification of novel *d* alleles uncovered by non-allelic methyltransferase mutations (Fig. 1; Hass et al. 2006). The phenotypic effects of the partial loss- or gain-of-function *d* alleles transmitted by R112,

B109, and NMS373 were masked by m^+ alleles—m^+ m^+ g^+ g^+ *d d* inbred lines produced wildtype tocopherol profiles (> 90% α-T) and were phenotypically indistinguishable from m^+ m^+ g^+ g^+ d^+ d^+ inbred lines (Table 1). The α-T percentage for NMS373 (95.8%) was close to the upper end of the phenotypic range (96.7% α-T) among the wildtype inbred lines we screened (Table 1; Hass et al. 2006). The presence or absence of strong *MT-2* alleles (d^+) might underlie subtle continuous differences in α-T percentage among wildtype inbred lines. Unless the effects of *MT-2* are completely masked by strong wildtype *MT-1* alleles, α-T percentages in g^+ g^+ or γ-T percentages in *g g* inbred lines might be maximized by identifying and selecting strong *MT-2* alleles. We did not specifically screen for d^+ alleles or identify or develop m^+ m^+ g^+ g^+ d^+ d^+ inbred lines. The d^+ allele we identified originated in LG24 (Demurin 1993; Demurin et al. 1996). We suspect other cryptic *d* alleles are floating around in wildtype germplasm. Such alleles are difficult if not impossible to identify phenotypically (without producing populations segregating for non-allelic mutations), but can be identified through quantitative transcript profiling (Fig. 7), allele resequencing (Supplemental Figs. S1, S2), and TILLING or ECOTILLING (Till et al. 2003; Comai et al. 2004; Comai and Henikoff 2006) and, if identified, might produce even more extreme phenotypes than have been identified so far.

When *MT-1* and *MT-2* were homozygous for mutant alleles (*m m* g^+ g^+ *d d*), flow through the MPBQ ⇒ DMPBQ ⇒ γ-T ⇒ α-T branch of the pathway was diminished and flow through the MPBQ ⇒ δ-T ⇒ β-T branch of the pathway was enhanced—α-T percentages ranged from 24.0 to 45.1 and β-T percentages ranged from 54.9 to 74.1 among *m m* g^+ g^+ *d d* inbred lines (Table 1; Hass et al. 2006). The tocopherol profiles of the latter were consistent with greatly diminished MPBQ/MSBQ-MT activities (Cheng et al. 2003; Van Eenennaam et al. 2003). Using allele sequences, INDEL marker genotypes, and biochemical phenotypes, several *m m* g^+ g^+ *d d* inbred lines were identified (B109, R112, MB17, VHB18, and VHB45) and had tocopherol phenotypes either close or virtually identical to the tocopherol phenotype for IAST-5 (Velasco et al. 2004b; Hass et al. 2006; Table 1); hence, IAST-5 has the biochemical phenotype predicted for diminished MPBQ/MSBQ-MT activity (Cheng et al. 2003; Van Eenennaam et al. 2003) and could harbor a novel *MT-1* or *MT-2* mutation.

α- and β-T synthesis was disrupted and γ- and δ-T synthesis was enhanced in lines carrying null *MT-1* and γ-*TMT* alleles (*m m g g* d^+ d^+), (Table 1; Fig. 1). The phenotype for the *m m g g* d^+ d^+ inbred line (HG81) was analogous to the phenotype for SRA16 (*m m* g^+ g^+ d^+ d^+): flow through the MPBQ ⇒ DMPBQ ⇒ γ-T branch of the pathway was diminished, whereas flow through the MPBQ ⇒ δ-T branch of the pathway was enhanced in HG81, the double null mutant (Table 1). Finally, when *MT-1*, *MT-2*, and γ-*TMT* were homozygous for mutant alleles (*m m g g d d*), α- and β-T synthesis were disrupted and γ- and δ-T synthesis were enhanced (Table 1). δ-T percentages were twofold greater than γ-T percentages in the triple mutant and matched pathway predictions (Cheng et al. 2003). The tocopherol phenotypes for the triple mutant inbred line HD55 (32.7% γ- and 67.3% δ-T) and IAST-4 (34.3% γ- and 58.2% δ-T), an inbred line developed by Velasco et al. (2004b), were virtually identical; hence, IAST-4 could be a triple mutant. The growth, development, and reproduction of the single, double, and triple mutant individuals and inbred lines we isolated were normal; however, in-depth analyses of the physiological and metabolic consequences of the mutations are needed.

The knockout *MT-1* and partial loss-of-function *MT-2* alleles we identified shed some light on the functions of the *MPBQ/MSBQ-MT* paralogs in sunflower, although additional biochemical and functional analyses are needed. Knockout mutations of *MPBQ/MSBQ-MT* are lethal in species harboring a single *MPBQ/MSBQ-MT* locus (Cheng et al. 2003; Motohashi et al. 2003; Van Eenennaam et al. 2003). Unless sunflower carries an as yet unidentified *MPBQ/MSBQ-MT* paralog, the non-lethality of the *MT-1* knockout mutation suggests that MPBQ/MSBQ-MT-2 can methylate MSBQ to yield plastoquinone, in addition to methylating MPBQ to yield DMPBQ, and has the dual functionality of the plant methyltransferases first reported by Cheng et al. (2003). The synthesis of PQ, a lipid-soluble plastid-localized electron carrier, is vital for normal plant growth and development (Cook and Miles 1992), whereas the synthesis of γ- and α-T from DMPBQ can be disrupted without impairing plant growth and development when tocopherol biosynthesis is redirected through the MPBQ ⇒ δ-T ⇒ β-T branch of the pathway (Table 1; Cheng et. al. 2003; Hass et al. 2006). The disruption of DMPBQ synthesis by non-lethal *MPBQ/MSBQ-MT* mutations produces novel δ- and β-T phenotypes, apparently without adversely affect plant growth and development. While MT-2 seems to have the multifunctionality of the MPBQ/MSBQ-MT identified by Cheng et al. (2003) and may play the dominant role in PQ biosynthesis in sunflower, we did not perform the biochemical analyses or have the null *MT-2* mutations needed to assess the functionality of *MT-1* and thus cannot assert whether MT-1 methylates MSBQ. Clearly, MT-1 methylates MPBQ

and, when knocked out, yields tocopherol phenotypes predicted by the disruption of MPBQ ⇒ DMPBQ methylation (Cheng et al. 2003; Motohashi et al. 2003; Van Eenennaam et al. 2003).

Acknowledgments This work was supported by funding to S.J.K. from the National Research Initiative of the United States Department of Agriculture Cooperative State Research, Education, and Extension Service Plant Genome Program (Grant No. 2003-35300-15184), the Paul C. Berger Endowment at Oregon State University, the Georgia Research Alliance, and University of Georgia Research Foundation.

References

Baack EJ, Whitney KD, Rieseberg LH (2005) Hybridization and genome size evolution: timing and magnitude of nuclear DNA content increases in *Helianthus* homoploid hybrid species. New Phytol 167:321–333

Bennetzen JL (2000) Mechanisms and rates of genome expansion and contraction in flowering plants. Genetica 115:251–269 29–36

Bennetzen JL (2002) Transposable element contributions to plant gene and genome evolution. Plant Mol Biol 42:251–269

Bergmüller E, Porfirova S, Dörmann P (2003) Characterization of an *Arabidopsis* mutant deficient in γ-tocopherol methyltransferase. Plant Mol Biol 52:1181–1190

Bowen NJ, McDonald JF (2001) Drosophila euchromatic LTR-retrotransposons are much younger than the host species in which they reside. Genome Res 11:1527–1540

Brown JWS (1996) Arabidopsis intron mutations and pre-mRNA splicing. Plant J 10:771–780

Cheng S, Fockler C, Barnes W, Higuchi R (1994) Effective amplification of long targets from cloned inserts and human genomic DNA. Proc Natl Acad Sci USA 91:5695–5699

Cheng Z, Sattler S, Maeda H, Sakuragi Y, Bryant DA, DellaPenna D (2003) Highly divergent methyltransferases catalyze a conserved reaction in tocopherol and plastoquinone synthesis in cyanobacteria and photosynthetic eukaryotes. Plant Cell 15:2343–2356

Collakova E, DellaPenna D (2001) Isolation and functional analysis of homogentisate phytyltransferase from Synechocystis sp PCC 6803 and Arabidopsis. Plant Physiol 127:1113–1124

Comai L, Young K, Till BJ, Reynolds SH, Greene EA, Codomo CA, Enns LC, Johnson JE, Burtner C, Odden AR, Henikoff S (2004) Efficient discovery of DNA polymorphisms in natural populations by Ecotilling. Plant J 37:778–86

Comai L, Henikoff S (2006) TILLING: practical single-nucleotide mutation discovery. Plant J 45:684–94

Cook W, Miles D (1992) Nuclear mutations affecting plastoquinone accumulation in maize. Photosynth Res 31:99–111

Cui X, Hsiac AP, Liu F, Ashlockd DA, Wise RP, Schnable PS (2003) Alternative transcription initiation sites and polyadenylation sites are recruited during *Mu* suppression at the *rf2a* locus of maize. Genetics 163:685–698

Demurin Y (1993) Genetic variability of tocopherol composition in sunflower seeds. Helia 16:59–62

Demurin Y, Skoric D, Karlovic D (1996) Genetic variability of tocopherol composition in sunflower seeds as a basis of breeding for improved oil quality. Plant Breed 115:33–36

Demurin Y, Efimenko SG, Peretyagina TM (2004) Genetic identification of tocopherol mutations in sunflower. Helia 27:113–116

Dolde D, Vlahakis C, Hazebroek J (1999) Tocopherols in breeding lines and effects of plant location, fatty acid composition, and temperature during development. J Am Oil Chem Soc 76:349–355

Emanuelsson O, Nielsen H, von Heijne G (1999) ChloroP, a neural network-based method for predicting chloroplast transit peptides and their cleavage sites. Protein Sci 8:978–984

Feschotte C, Jiang N, Wessler SR (2002) Plant transposable elements: where genetics meets genomics. Nature Rev Genetics 3:329–341

Fick GN, Zimmer DE, Kinman ML (1974) Registration of six sunflower parental lines. Crop Sci 14:912

Grandbastein AM, Spielman A, Caboche M (1989) *Tnt1*, a mobile retroviral-like transposable element of tobacco isolated by plant cell genetics. Nature 337:376–380

Grandbastein AM (1998). Activation of plant retrotransposons under stress conditions. Trends Plant Sci. 3:181–187

Greene EA, Codomo CA, Taylor NE, Henikoff JG, Till BJ, Reynolds SH, Enns LC, Burtner C, Johnson JE, Odden AR, Comai L, Henikoff S (2003) Spectrum of chemically induced mutations from a large-scale reverse-genetic screen in Arabidopsis. Genetics 164:731–40

Grusak MA, DellaPenna D (1999) Improving the nutrient composition of plants to enhance human nutrition and health. Annu Rev Plant Physiol Plant Mol Biol 50:133–161

Hass CG, Leonard SW, Miller JF, Slabaugh MB, Traber MG, Knapp SJ (2003) Genetics of tocopherol (vitamin E) composition mutants in sunflower. In: Abstract of Plant and Animal Genome Conference XI, San Diego, CA, USA, Jan 11–15, 2003 (http://wwwintl-pagorg/11/ abstracts/P7b_P821_XI.html)

Hass CG, Tang S, Leonard S, Traber M, Miller JF, Knapp SJ (2006) Three non-allelic epistatically interacting methyltransferase mutations produce novel tocopherol (vitamin E) profiles in sunflower. Theor Appl Genet (in press)

Hoffmann GR (1980) Genetic effects of dimethyl sulfate, diethyl sulfate, and related compounds. Mutat Res 75:63–129

Jiang N, Feschotte C, Zhang X, Wessler SR (2004) Using rice to understand the origin and amplification of miniature inverted repeat transposable elements (MITEs). Curr Opin Plant Biol 7:115–119

Johns MA, Mottinger J, Freeling M (1985) A low copy number, *copia*-like transposon in maize. EMBO J 4:1093–1102

Joshi C, Chiang V (1998) Conserved sequence motifs in plant *S*-adenosyl-*L*-methionine-dependent methyltransferases. Plant Mol Biol 37:663–674

Kagan R, Clarke S (1994) Widespread occurrence of three sequence motifs in diverse *S*-adenosylmethionine-dependent methyltransferases suggests a common structure for these enzymes. Arch Biochem Biophys 310:417–427

Kamal-Eldin A, Andersson R (1997) A multivariate study of the correlation between tocopherols composition content and fatty acid composition in vegetable oils. J Am Oil Chem Soc 74:375–380

Lal SK, Choi J-H, Shaw JR, Hannah LC (1999) A splice site mutant of maize activates cryptic splice sites, elicits intron inclusion and exon exclusion, and permits branch point elucidation. Plant Physiol 121:411–418

Lal SK, Giroux MJ, Brendel V, Vallejos CE, Hannah LC (2003) The maize genome contains a *helitron* insertion. Plant Cell 15:381–391

Lal SK, Hannah LC (2005) Plant genomes: massive changes of the maize genome are caused by Helitrons. Heredity 95:421–2

Lander ES, Green P, Abrahamson J, Barlow A, Daly MJ, Lincoln SE, Newburg L (1987) MAPMAKER: an interactive computer package for constructing primary genetic linkage maps of experimental and natural populations. Genomics 1:174–181

Ma J, Devos KM, Bennetzen JL (2004) Analyses of LTR-retrotransposon structures reveal recent and rapid genomic DNA loss in rice. Genome Res 14:860–869

Marchler-Bauer A, Bryant SH (2004) CD-Search: protein domain annotations on the fly. Nucleic Acids Res 32:W327–W331

Marillonnet S, Wessler SR (1997) Retrotransposon insertion into the maize waxy gene results in tissue-specific RNA processing. Plant Cell 9:967–78

Marillonnet S, Wessler SR (1998) Extreme structural heterogeneity among the members of a maize retrotransposon family. Genetics 150:1245–56

Michelmore RW, Paran I, Kesseli V (1991) Identification of markers linked to disease resistance genes by bulked segregant analysis: a rapid method to detect markers in specific genomic regions by using segregating populations. Proc Natl Acad Sci USA 88:9828–9832

Miller JF (1997) Registration of cms HA89 (PEF1) cytoplasmic male-sterile, RPEF1 restorer, and two nuclear male-sterile (NMS373 and 377) sunflower genetic stocks. Crop Sci 37:1984

Motohashi R, Ito T, Kobayashi M, Taji T, Nagata N, Asami T, Yoshida S, Yamaguchi-Shinozaki K, Shinozaki K (2003) Functional analysis of the 37 kDa inner envelope membrane polypeptide in chloroplast biogenesis using a *Ds*-tagged Arabidopsis pale-green mutant. Plant J 34:719–731

Perez-Vich B, Berry ST, Velasco L, Fernandez-Martinez JM, Gandhi S, Freeman C, Heesacker A, Knapp SJ, Leon AJ (2005) Molecular mapping of nuclear male sterility genes in sunflower. Crop Sci 45:1851–1857

Porfirova S, Bergmüller E, Tropf S, Lemke R, Dormann P (2002) Isolation of an Arabidopsis mutant lacking vitamin E and identification of a cyclase essential for all tocopherol biosynthesis. Proc Natl Acad Sci USA 99:12495–12500

Purugganan MD, Wessler SR (1994) Molecular evolution of *magellan*, a maize *Ty3*/*gypsy*-like retrotransposon. Proc Natl Acad Sci USA 91:11674–11678

Roath WW, Miller JF, Gulya TJ (1981) Registration of RHA 801 sunflower germplasm. Crop Sci 21:479

Rocheford TR, Wong JC, Egesel CO, Lambert RJ (2002) Enhancement of vitamin E levels in corn. J Am Coll Nutr 21:191S–198S

Rozas J, Sanchez-Delbarrio JC, Messeguer X, Rozas R (2003) DnaSP, DNA polymorphism analyses by the coalescent and other methods. Bioinformatics 19:2496–2497

SanMiguel P, Tikhonov A, Jin YK, Motchoulskaia N, Zakharov D, Melake-Berhan A, Springer PS, Edwards KJ, Lee M, Avramova Z, Bennetzen JL (1996) Nested retrotransposons in the intergenic regions of the maize genome. Science 274:765–768

SanMiguel P, Gaut BS, Tikhonov A, Nakajima Y, Bennetzen JL (1998) The paleontology of intergene retrotransposons of maize. Nature Genet 20:43–45

Santini S, Cavallini A, Natali L, Minelli S, Maggini F, Cionini PG (2002) *Ty1/copia*- and *Ty3/ gypsy*-like DNA sequences in Helianthus species. Chromosoma 111:192–120

Sattler SE, Cahoon EB, Coughlan SJ, DellaPenna D (2003) Characterization of tocopherol cyclases from higher plants and cyanobacteria: evolutionary implications for tocopherol synthesis and function. Plant Physiol 132:2184–2195

Sattler SE, Gillilanda LU, Magallanes-Lundbacka M, Pollard M, DellaPenna D (2004) Vitamin E is essential for seed longevity and for preventing lipid peroxidation during germination. Plant Cell 16:1419–1432

Sheppard AJ, Pennington JAT, Weihrauch JL (1993) Analysis and distribution of vitamin E in vegetable oils and foods. In: Packer L, Fuch J (eds) Vitamin E in health and disease. Marcel-Dekker, New York, pp 9–31

Shintani DK, DellaPenna D (1998) Elevating the vitamin E content of plants through metabolic engineering. Science 282:2098–2100

Shintani DK, Cheng Z, DellaPenna D (2002) The role of 2-methyl-6-phytylbenzoquinone methyltransferase in determining tocopherol composition in *Synechocystis* sp. PCC6803. FEBS Lett. 511:1–5

Song SU, Gerasimova T, Kurkulos M, Boeke JD, Corces VG (1994) An env-like protein encoded by a Drosophila retroelement: evidence that gypsy is an infectious retrovirus. Genes Dev 8:2046–2057

Tang S, Yu JK, Slabaugh MB, Shintani DK, Knapp SJ (2002) Simple sequence repeat map of the sunflower genome. Theor Appl Genet 105:1124–1136

Tang S, Kishore VK, Knapp SJ (2003) PCR-multiplexes for a genome-wide framework of simple sequence repeat marker loci in cultivated sunflower. Theor Appl Genet 107:6–19

Tang S, Hass CG, Knapp SJ (2005) Candidate genes for mutations causing changes in tocopherol composition in sunflower. In: Abstract of Plant and Animal Genome Conference XIII, San Diego, CA, USA, Jan 15–19, 2005 (http://www.intl-pag.org/13/abstracts/PAG13_W071.html)

Tatusova TA, Madden TL (1999) Blast 2 sequences - a new tool for comparing protein and nucleotide sequences. FEMS Microbiol Lett 174:247–250

Thompson JD, Higgins DG, Gibson TJ (1994) CLUSTAL W: improving the sensitivity of progressive multiple sequence alignment through sequence weighting, position-specific gap penalties and weight matrix choice. Nucleic Acids Res 22:4673–4680

Till BJ, Reynolds SH, Greene EA, Codomo CA, Enns LC, Johnson JE, Burtner C, Odden AR, Young K, Taylor NE, Henikoff JG, Comai L, Henikoff S (2003) Large-scale discovery of induced point mutations with high-throughput TILLING. Genome Res 13:524–30

Van Eenennaam AL, Lincoln K, Durrett TP, Valentin HE, Shewmaker CK, Thorne GM, Jiang J, Baszis SR, Levering CK, Aasen ED, Hao M, Stein JC, Norris SR, Last RL (2003) Engineering vitamin E content: from Arabidopsis mutant to soy oil. Plant Cell 15:3007–3019

Varagona MJ, Purugganan M, Wessler SR (1992) Alternative splicing induced by insertion of retrotransposons into the maize *waxy* gene. Plant Cell 4:811–820

Velasco L, Domínguez J, Fernández-Martínez JM (2004a) Registration of T589 and T2100 sunflower germplasms with modified tocopherol profiles. Crop Sci 44:362–363

Velasco L, Pérez-Vich B, Fernández-Martínez JM (2004b) Novel variation for the tocopherol profile in a sunflower created by mutagenesis and recombination. Plant Breed 123:490–492

Weil CF, Marillonnet S, Burr B, Wessler SR (1992) Changes in state of the *Wx-m5* allele of maize are due to intragenic transposition of *Ds*. Genetics 130:75–85

Wong JC, Lambert RT, Tadmor Y, Rocheford TR (2003) QTL associated with accumulation of tocopherols in maize. Crop Sci 43:2257–2266

Yu JK, Tang S, Slabaugh MB, Heesacker A, Cole G, Herring M, Soper J, Han F, Chu WC, Webb DM, Thompson L, Edwards KJ, Berry S, Leon AJ, Olungu C, Maes N, Knapp SJ (2003) Towards a saturated molecular genetic linkage map for cultivated sunflower. Crop Sci 43:367–387